

# Catalytic Activities of Various Moderately Strong Solid Acids and Their Correlation with Surface Polarity Parameters

Simone Adolph, Stefan Spange,\* and Yvonne Zimmermann

Department of Polymer Chemistry, Institute of Chemistry, University of Technology Chemnitz, Strasse der Nationen 62, 09107 Chemnitz, Germany

Received: February 21, 2000

The specific rate constant  $k'$  of the surface-mediated hydride-transfer reaction of 1,4-cyclohexadiene with triphenylmethyl cation is strongly dependent on the nature of the solid acid catalyst used. The catalysis of this hydride-transfer reaction by 30-moderately strong solid acid catalysts, e.g., silicas, aluminas, aluminosilicates, and titanium dioxide particles, has been studied. Generation of the triphenylmethyl cation when chlorotriphenylmethane is chemisorbed to the solid acid catalyst was used for the kinetic measurement. The individual, pseudo-first-order rate constant,  $k$ , of the hydride-transfer reaction increases linearly with the amount of solid acid catalyst used. The specific rate constant,  $k'$ , based on the surface area of the solid acid, was used to quantify the catalytic activity of the solid acids.  $k'$  increases in the order silicas < aluminosilicates < titanium dioxides  $\approx$  aluminas.  $\ln k'$  can be correlated with the corresponding surface polarity parameters of the solid acid, e.g., Reichardt's  $E_T(30)$ , Gutmann's acceptor number AN, and Kamlet–Taft's parameters  $\alpha$  (hydrogen-bond-donating acidity) and  $\pi^*$  (dipolarity/polarizability). It is shown that the catalytic activity of a moderately strong solid acid catalyst can be characterized by Gutmann's acceptor number AN or the Kamlet–Taft  $\alpha$  value. The different classes of solid acids, e.g., silicas, aluminas, and aluminosilicates, respectively, give different dependencies of  $k'$  as a function of their solid acid acidity parameters.

## Introduction

The catalytic activity of common solid acids, e.g., various silicas, aluminas, titanium dioxides, and aluminosilicates, often specifically depends on the experimental pretreatment used for the process to be catalyzed.<sup>1–3</sup> Thus, a thermal pretreatment of silica above 250 °C decreases its surface polarity because silanol groups are converted into siloxane bridges.<sup>4,5</sup> Also, residual amounts of water on the surface influence polarity and catalytic activity of solid acids as a whole in a very complex manner.<sup>6–8</sup> Solid-state NMR spectroscopy and calorimetry were successfully used for investigating the acidity of a series of strong and moderately strong solid acid catalysts, e.g., silica,<sup>8</sup>  $\text{HPWO}_3$ ,<sup>9</sup> silica– $\text{OAlCl}_2$ ,<sup>10,11</sup> HZSM 5,<sup>12,13</sup> and other zeolites,<sup>12,13</sup> and their interaction with bases.

Rapid methods for the detection of differences of the surface acidity make use of Hammett indicators<sup>1,14,15</sup> or solvatochromic dyes.<sup>16–19</sup> The dyes are adsorbed on the solid acid catalyst and then measured by UV/vis spectroscopic techniques. Several relationships are reported between the Hammett acidity function of solid acid surfaces and catalytic processes.<sup>1,15</sup> However, Hammett indicators, which are classical acid–base indicators, have some inadequacies because they measure only distinct differences in the frame of the Hammett ( $H_0$ ) acidity scale. Different aluminosilicates and silicas with different acidities often cannot be distinguished by Hammett indicators.<sup>15,16</sup> With genuine solvatochromic dyes, one can distinguish very small differences in the polarity of solvents.<sup>20,21</sup> They are also suitable for analyzing the polarity of surfaces of organically functionalized silica particles<sup>17a,18,22,23</sup> and various inorganic solid acids.<sup>22c</sup>

The following solvatochromic probe molecules have been well-established as surface polarity indicators for several ap-

plications during the recent years: 2,6-diphenyl-4-(2,4,6-triphenyl-1-pyridinio)phenolate (**1a**), Reichardt's standard dye, and an eicosa fluorine-substituted derivative of **1a** (**1b**) that is especially useful for moderately acidic solvents,<sup>22c,24</sup>  $\text{Fe}(\text{phen})_2(\text{CN})_2$  [iron(II)-dicyano-bis(1,10)-phenanthroline] (**2**),<sup>25,26</sup> and Michler's ketone [4,4'-bis-(*N,N*-dimethylamino)benzophenone] (**3**).<sup>25</sup> Indicator formulas are given below in Chart 3. The position of the UV/vis absorption maximum of the adsorbed dye [ $\nu_{\text{max}}(\text{indicator})$ ] was used as units for surface polarity. For instance, the molar absorption energy of the UV/vis maxima of **1a**, expressed as  $\text{kcal mol}^{-1}$ , is the equivalent of the well-known Reichardt's  $E_T(30)$  polarity scale (eq 1).<sup>20,21</sup>

$$E_T(30) [\text{kcal mol}^{-1}] = 2.8951 \times 10^{-3} \nu_{\text{max}}(\mathbf{1a}) [\text{cm}^{-1}] \quad (1)$$

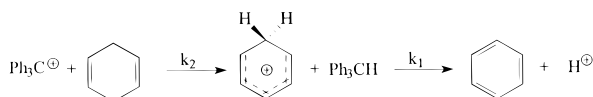
Kamlet–Taft's solvent parameters  $\alpha$ ,  $\beta$ , and  $\pi^*$ <sup>27</sup> are recommended by several authors as very useful for describing processes at the solid/liquid as well as solid/gaseous interface.<sup>28–30</sup> The  $\alpha$  and  $\pi^*$  values for various micelles<sup>31</sup> and solid surfaces<sup>22,25b</sup> were determined by means of LSE (linear solvation energy)<sup>20,21,31</sup> relationships using the Kamlet–Taft solvent parameters as a reference system. The simplified Kamlet–Taft equation applied to solvatochromic shifts [ $\text{XYZ} = \nu_{\text{max}}(\text{indicator})$ ] is given in eq 2.<sup>20,32</sup>

$$\text{XYZ} = (\text{XYZ})_0 + a\alpha + b\beta + s(\pi^* + d\delta) \quad (2)$$

$(\text{XYZ})_0$  is the value for the solvent reference system, either a nonpolar medium or the gas phase,  $\alpha$  describes the HBD (hydrogen-bond-donating) ability,  $\beta$  is the HBA (hydrogen-bond-accepting) ability, and  $\pi^*$  is the dipolarity/polarizability of the solvents.  $\delta$  is a polarizability correction term that is 1.0

\* Corresponding author.

### CHART 1. Hydride-Transfer Reaction of 1,4-Cyclohexadiene with Surface-Coordinated Triphenylmethylium



for aromatic, 0.5 for polyhalogenated, and zero for aliphatic solvents; *a*, *b*, *s*, and *d* are solvent-independent coefficients.<sup>25</sup>

In the previous paper we reported on the determination of the Kamlet–Taft  $\alpha$  and  $\pi^*$  values for more than 30 solid acid catalysts by means of the indicators **2** and **3**.<sup>22c</sup> In the same paper, values of the Reichardt's  $E_T(30)$  polarity parameter of the solid acids were directly determined by the dyes **1a** and **1b**. However, the solvatochromic indicators **1a**, **1b**, **2**, and **3** are moderately weak bases.<sup>32,33</sup> For the solvatochromic measurements, very low concentrations of the indicators are used to avoid multilayer adsorption on the surface. It is assumed that the strongest acidic sites preferentially interact at low dye concentration, but the energies are average energies of all the sites to which a base coordinates. This average energy is a measure of the acid strength or polarity strength of the strongest site only if just the strongest site interacts. Therefore, it is of great interest to evaluate the relevance of the calculated polarity parameters  $E_T(30)$ ,  $\alpha$ , and  $\pi^*$  with regard to the catalytic activity of the solid acid catalyst.

Ammonia, substituted amines, or acetone is often used as a probe in evaluating the surface acidity for zeolites.<sup>1–12,34,35</sup> These probes are small and can penetrate into the channels and pores of the solid acid materials. It is obvious that the surface polarity indicators **1a**, **1b**, and **2** are large. They cannot penetrate into channels of a Y-zeolite or ZSM 5 materials. Therefore, these polarity indicators can only observe the external solid surface of aluminosilicate cages and the polarity within large pores with a diameter size > 1 nm.

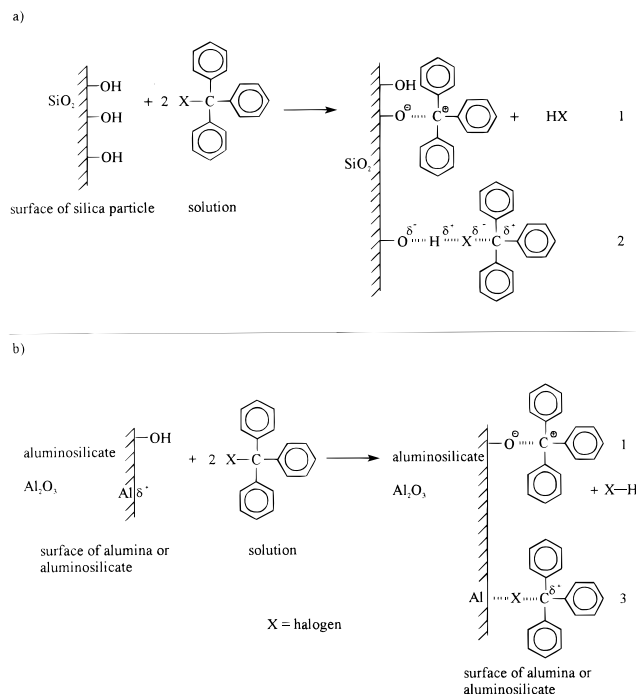
Accordingly, we established the following conditions for testing the catalytic activity of common solid acids.

- (1) The substrate should be activated by the solid acid, but the reagent should not be affected by the solid acid catalyst.
- (2) The substrate (precursor) should be of similar size as the surface polarity indicator.
- (3) The educts (substrate and reagent) should not react in the surrounding solution phase.
- (4) The products should also not affect the catalytic activity of the solid acid catalyst.
- (5) The rate of the elementary step in the model reaction should be the rate-determining step. Rate of adsorption of the educts and desorption of the products should be faster than the model reaction.

All the desired conditions are satisfied by the surface-mediated hydride-transfer reaction of 1,4-cyclohexadiene (CHD), as the reagent, with  $(C_6H_5)_3C^+$  that can be generated by chemisorption of  $(C_6H_5)_3CCl$  on silicas, aluminas, titanium dioxides, or aluminosilicates.<sup>36</sup> The hydride-transfer reaction of CHD with  $(C_6H_5)_3C^+ BF_4^-$  in dichloromethane solution as well as that of CHD with chemisorbed  $(C_6H_5)_3C^+$  on solid acids yield quantitatively  $(C_6H_5)_3CH$  and benzene (Chart 1).<sup>37–39</sup>

It is expected that the catalyst affects the reactivity of the  $(C_6H_5)_3C^+$  and the short-lived CHD carbenium intermediate (the benzenonium ion,  $C_6H_7^+$ ). The benzenonium intermediate has a strong Brønsted acidity ( $pK_{RH^+} = -24$ ). Therefore, the proton-transfer reaction should occur faster than the first step, the hydride-ion-transfer reaction.

### CHART 2. Proposed Adsorption-Ionization Mechanisms of Chlorotriphenylmethane on Silica and/or Alumina Surface Sites

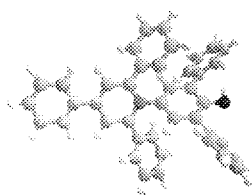


The reaction to be catalyzed by means of solid acid catalysts shown in Chart 1 has been chosen for the reasons 1–5 given above. Preliminary experiments showed that mixtures of CHD and  $(C_6H_5)_3CCl$  remain stable in a pure solution of dichloromethane. CHD is also stable in the presence of the solid acid catalyst in dichloromethane over a time period suitable for the model reaction. No side reactions occur if any component is absent.  $(C_6H_5)_3CCl$  was used as the  $(C_6H_5)_3C^+$  precursor because it can be easily activated on each solid acid catalyst studied.

During the last three decades, the mechanism of heterolytic dissociation of arylmethyl compounds for producing carbenium ions on solid acids was studied by several authors.<sup>36,38,40–43</sup> In the year 1939, Weitz first reported that chlorotriphenylmethane becomes yellow-colored when adsorbed on silica from a benzene solution.<sup>40</sup> Leftin studied the chemisorption of various triphenylmethane derivatives on aluminosilicates.<sup>36</sup> Other authors studied the infrared, UV/vis, and  $^1H$  MAS NMR spectra of these adsorbates.<sup>41,42,43</sup> Recently, “ship in the bottle” synthesis of substituted triarylmethyl cations in HY-zeolites were also reported by several authors.<sup>44–46</sup> Despite the well-documented chemisorption process of chlorotriphenylmethane to silica,<sup>36,40–43</sup> some questions remain whether a halide–carbenium ion pair or a silanolate–carbenium ion pair is present on silica. We believe that different kinds of species can be present owing to the reversible temperature dependence of the  $(C_6H_5)_3CCl$  adsorption–ionization equilibrium (Chart 2).<sup>47</sup>

Thus,  $(C_6H_5)_3CCl$  chemisorbed on solid acids is present in an equilibrium state similar to its heterolytic dissociation, which is caused by weak Lewis acids ( $ZnCl_2$ ,  $SbCl_3$ ) or acceptor solvents.<sup>48–50</sup>

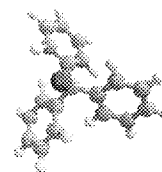
Despite some open questions about the details, chlorotriphenylmethane adsorbed on silica reacts quantitatively with CHD to benzene and triphenylmethane. In ref 38b we have already mentioned that chlorodiarylmethanes analogously react with CHD on silica. The HCl formed does not significantly accelerate the reaction rate. Benzene as product and CHD as

**CHART 3. Comparison of the Sizes of the Surface Polarity Indicators 1A and 3 with That of Chlorotriphenylmethane**

2,6-diphenyl-4-(2,4,6-triphenyl-1-pyridinio)phenolate



Michler's Ketone



Chlorotriphenylmethane

**CHART 4. Drawing That Shows the General Problem to Be Investigated**

<p>UV/Vis spectroscopic detection solvatochromic shift <math>\nu_{\max}(S)</math> polarity parameters: <math>\alpha</math>, <math>\pi^*</math>, AN, <math>E_T(30)</math></p>	<p>kinetic measurement <math>\lg k'</math></p>
(S) Solvatochromic probe dye	(R) Reagent

Question: How does  $\lg k'$  correlate with the values of the polarity parameters?

educt can be simultaneously detected by a gas chromatograph (GC) (see Experimental Section).

The comparison of the sizes of two polarity indicators with that of the substrate  $(C_6H_5)_3CCl$  for the model reaction shows that both groups of compounds are similar. This is illustrated in Chart 3.

Thus, it is expected that the relevant structure of the surface acidic sites that are observed by the two different types of compounds is of similar geometry and size, for both the triphenylmethyl cation precursor and the solvatochromic probes. The problem investigated in the present paper is shown in Chart 4.

We expect to answer the following question: Is it possible to find a reasonable correlation between data derived from UV/vis spectroscopy of solvatochromic probe dye indicators, analyzed by LSE relationships,<sup>22c</sup> and kinetic data from a polar model reaction on the solid acid catalysts?

For this study we used a selection of the same moderately strong solid acid samples as investigated in the previous paper.<sup>22c</sup> The acidity of the solids ranges on the Hammett acidity scale between  $H_0 = 4.4$  (Aerosil 300) and  $H_0 = -9.3$  and  $-10.5$  (aluminosilicates) and on the Kamlet-Taft HBD scale between  $\alpha = 1$  (silicas) and  $\alpha = 1.9$  (aluminosilicates). It should be mentioned that the Hammett acidities ( $H_0$  value) of the solids do not correlate well with the Kamlet-Taft  $\alpha$  value.

**Experimental Section**

**Materials.** The chemical composition and physical properties of the solid acid catalysts used are summarized in Table 1. They were either commercially available products or synthesized by the procedure given in ref 22c as indicated in Table 1.

Triphenylmethanol (Merck) was recrystallized from benzene before use.

Chlorotriphenylmethane and bromotriphenylmethane (Merck) were recrystallized from a benzene/hexane (20/80) mixture that contains 2% acetyl chloride and bromide, respectively.

Triphenylmethyl isothiocyanate was synthesized from chlorotriphenylmethane and sodium rhodanide in acetone as solvent.<sup>51</sup>

1,4-Cyclohexadiene was purchased from Merck, dried over  $CaH_2$  and purity checked by GC (gas chromatography), before use.

Dichloromethane (Merck, analytical grade) was freshly distilled over  $CaH_2$  and stored under dried argon.

**Kinetic Measurements.** A measured amount of the solid acid catalyst was heated at 400 °C for 12 h and then allowed to cool to room temperature under dried argon. This portion of the thermally activated catalyst was put in a glass flask and suspended in 25 mL of dried dichloromethane. Chlorotriphenylmethane (0.0020 mol) and 100  $\mu$ L of toluene, as the internal standard for the GC, were added to the suspension of the solid acid catalyst. By pouring 100  $\mu$ L of 1,4-cyclohexadiene ( $n_{CHD} = 0.0011$  mol) into the suspension, the reaction was started. During the reaction, the suspension was continually shaken and kept at 295 K in a thermostat. The reaction was followed by analyzing the surrounding organic phase using a gas chromatograph (GC-14B, Shimadzu) provided with a 25 m capillary column of 5% phenylmethylsilicone. A typical kinetic plot is shown below in Figure 5.

For the silicas, a hydride-transfer reaction takes also place in the surrounding solution phase when the solid was separated because the silica particles and an excess of chlorotriphenylmethane yield  $(C_6H_5)_3C^+ HCl_2^-$ . However, this simultaneous hydride-transfer reaction in the surrounding solution occurs very slowly and does not affect determination of the rate constant for the heterogeneously mediated reaction.<sup>47b</sup>

**UV/Vis Spectroscopic Measurements. Absorption Spectroscopy.** The UV/vis absorption maxima of the triphenylmethyl compounds adsorbed on the solid acid catalyst were recorded using a diode array UV/vis spectrometer (MCS 4 Carl Zeiss) with glass fiber optics. The concentration of the triphenylmethyl compound was about 1–10 mg per gram of catalyst. The transparent silica/1.2-dichloroethane suspensions were measured as previously reported.<sup>22</sup> UV/vis spectra of nontransparent suspensions of alumina, titanium dioxide, and the other solids were recorded by a special reflectance technique. A quartz plate is used as the bottom of the closed measuring cell containing the suspension. The sensor head for measuring the reflectance spectra is located at this quartz plate, and the UV/vis spectrum of the adsorbed dye can be monitored after the particles deposit on the plate. This technique is very suitable for recording UV/vis spectra of nontransparent particles in suspensions under inert conditions.<sup>22c</sup> The reproducibility of the UV/vis spectra is very good. The measurement error of the UV/vis absorption maxima of triphenylmethyl cation adsorbed onto aluminas, aluminosilicates, or titanium dioxides is  $\lambda_{\max} \pm 2$  nm using the reflectance technique. For the silicas, a transparent suspension is obtained

**TABLE 1: Solid Acids Used in This Paper, Their Chemical Compositions, and Physical Properties**

sample no.	solid acid sample	BET surface area (m <sup>2</sup> g <sup>-1</sup> )	specific pore volume (cm <sup>3</sup> g <sup>-1</sup> )	average pore diameter (nm)	source
1	SiO <sub>2</sub> , KG 60	423	0.63	9.0	Merck
2	SiO <sub>2</sub> , SG 432	315	1.42	n.d. <sup>a</sup>	Grace
3	SiO <sub>2</sub> , LC 1500	30	n.d. <sup>a</sup>	5.5	Grace
4	SiO <sub>2</sub> , SP 18–8470	776	0.57	4.5	Grace
5	SiO <sub>2</sub> , Aerosil 300	240			Gegussa
6	Al <sub>2</sub> O <sub>3</sub>	97	0.50	10.3	Condea
7	Al <sub>2</sub> O <sub>3</sub> , Tonerdekugeln	160	0.40		Condea
8	Al <sub>2</sub> O <sub>3</sub> , SP 18–8510	131	0.72		Grace
9	Al <sub>2</sub> O <sub>3</sub> –C	100	0.57	11.4	Degussa
10	Al <sub>2</sub> O <sub>3</sub> (AlEt <sub>2</sub> Cl)	58	0.17	5.9	<i>b</i>
11	Al <sub>2</sub> O <sub>3</sub> , Pural SB	292	0.54	2.7	Condea
12	aluminosilicate, Siral 5	296	0.46	3.1	Condea
13	aluminosilicate, Siral 10	347	0.44	2.5	Condea
14	aluminosilicate, Siral 20	315	0.35	2.2	Condea
15	aluminosilicate, Siral 30	351	0.36	2.1	Condea
16	aluminosilicate, Siral 40 (S2036)	490			Condea
17	aluminosilicate, Siral 40 (S2042)	468			Condea
18	aluminosilicate, Siral 40 (S2045)	499			Condea
19	aluminosilicate, Siral 40 (S2331)	476			Condea
20	aluminosilicate, Siral 40 (S2334)	432			Condea
21	aluminosilicate, Siral 40 (S2386)	489	0.83		Condea
22	aluminosilicate, Siral 40 (S2390)	468	0.78		Condea
23	aluminosilicate, Siral 50	381	0.50	2.6	Condea
24	aluminosilicate, Siral 60	356	0.34	1.9	Condea
25	aluminosilicate, Siral 80	263	0.42	3.2	Condea
26	TiO <sub>2</sub> P25	52	0.27	10.0	Degussa
27	TiO <sub>2</sub> (Rutil)	30	0.14	9.3	Condea
28	TiO <sub>2</sub> (Anatas)	45	0.16	7.1	Condea
29	AlPO <sub>4</sub> , SP 8293	254	0.57	6.4	Grace
30	Al <sub>2</sub> O <sub>3</sub> /SiO <sub>2</sub> , SP 2–8515.01	336	0.80	4.8	Grace
31	TiO <sub>2</sub> /SiO <sub>2</sub> , SP 18–8381.01	303	1.22	1.5	Grace
32	KG 60 10% Al <sub>2</sub> O <sub>3</sub>	413	0.79	3.8	<i>b</i>
33	KG 60 30% Al <sub>2</sub> O <sub>3</sub>	354	0.78	4.4	<i>b</i>
34	KG 60 50% Al <sub>2</sub> O <sub>3</sub>	344	0.74	4.3	<i>b</i>
35	KG 60 70% Al <sub>2</sub> O <sub>3</sub>	361	0.77	4.3	<i>b</i>
36	KG 60 100% Al <sub>2</sub> O <sub>3</sub>	339	0.56	3.3	<i>b</i>

<sup>a</sup> Not determined. <sup>b</sup> See ref 22c, experimental part. Grafted with aluminumdiethyl chloride (AlEt<sub>2</sub>Cl) and hydrolyzed with water; the 10% means that 10% Al<sub>2</sub>O<sub>3</sub> is produced per amount silica.

in 1,2-dichloroethane as liquid. This permits good quality transmission spectra with excellent reproducibility less than  $\lambda_{\text{max}} \pm 1$  nm.

Surface titration of Aerosil 300 with chlorotriphenylmethane was carried out directly in the slurry. The stock solution of chlorotriphenylmethane was added by glass syringe through a silicone septum. The spectra were recorded immediately by an immersion cell (TSM 5) that was placed directly in the slurry.

Three runs were done for each solid acid. For correcting the intensity of the triphenylmethylium UV/vis absorption on the silica surface at  $\lambda_{\text{max}} = 435$  nm, amounts of nonadsorbed triphenylmethylium species can be detected in the supernatant solution after the particles are deposited.

**Fluorescence Spectroscopy.** For the fluorescence measurements of the slurry, the reflectance technique (Shimadzu) was used. The incident angle is 30°, and the detection angle is 60° for reflected light.

**BET Measurements.** The BET surface area was measured with N<sub>2</sub> at 77 K using a Sorptomatik 1900 (Fisons).

**Correlation Analyses.** The correlation analyses were done with the statistics program Microcal Origin version 5.0 SR2 from Microcal Software.

## Results

**UV/Vis Spectroscopy.** As mentioned, the covalent compound (C<sub>6</sub>H<sub>5</sub>)<sub>3</sub>CCl becomes cationically active when adsorbed to the solid acids (see Table 1). The UV/vis absorption of (C<sub>6</sub>H<sub>5</sub>)<sub>3</sub>C<sup>+</sup> on the surface of the solid acid catalyst at  $\lambda_{\text{max}} = 412/435$  nm

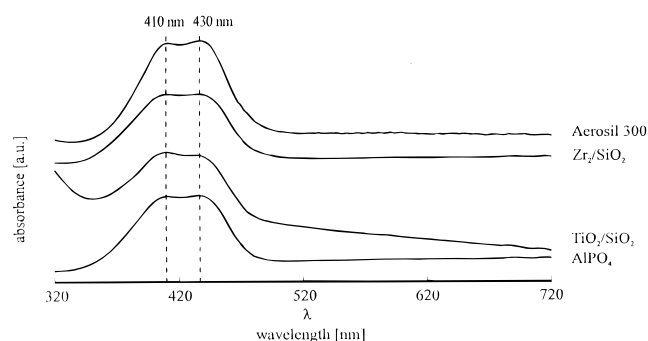


**Figure 1.** UV/vis spectra of chemisorbed chlorotriphenylmethane measured in the slurry of different solid acid particles, e.g., Aerosil 300, TiO<sub>2</sub>/SiO<sub>2</sub>, ZrO<sub>2</sub>/SiO<sub>2</sub>, and AlPO<sub>4</sub>, by the transmission technique in dichloromethane at room temperature.

can be monitored by UV/vis spectroscopy.<sup>48,49</sup> Characteristic UV/vis spectra of (C<sub>6</sub>H<sub>5</sub>)<sub>3</sub>C<sup>+</sup>, when (C<sub>6</sub>H<sub>5</sub>)<sub>3</sub>CCl is adsorbed on some solid acids, are shown in Figure 1.

It should be noted that the absorption maximum of the chemisorbed triphenylmethylium at  $\lambda_{\text{max}} = 412/435$  nm is unaffected by the nature of the solid acid catalyst. This result is consistent with related literature results. They report that the nature of the solvent or counterion does not change the position of the (C<sub>6</sub>H<sub>5</sub>)<sub>3</sub>C<sup>+</sup> UV/vis absorption maximum at  $\lambda_{\text{max}} = 410/430$  nm.<sup>48,49</sup> In the case of the titanium dioxide particles, care must be taken because visible light causes a photochemical reaction of the triphenylmethylium that gives a reddish color



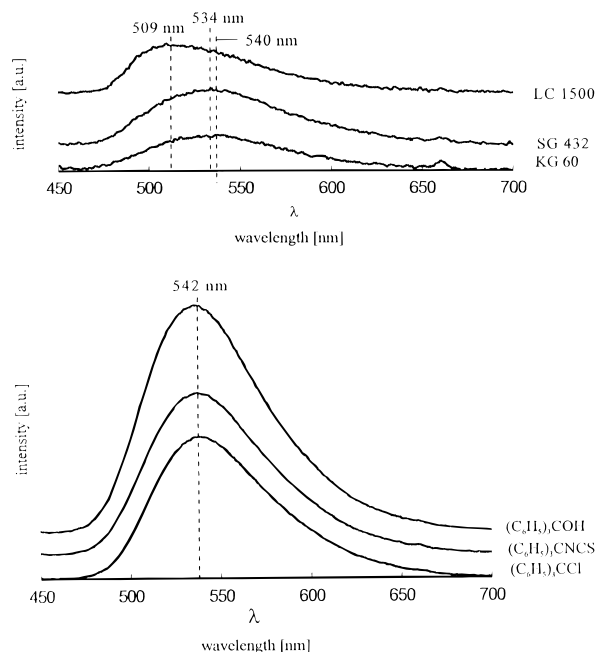


**Figure 2.** (a, top) UV/vis fluorescence spectra of chemisorbed chlorotriphenylmethane on different solid acids in 1,2-dichloroethane at room temperature. The excitation wavelength was  $\lambda = 456$  nm. (b, bottom) UV/vis fluorescence spectra of chemisorbed  $(\text{C}_6\text{H}_5)_3\text{COH}$ ,  $(\text{C}_6\text{H}_5)_3\text{CCl}$ , and  $(\text{C}_6\text{H}_5)_3\text{CNCS}$  measured on an aluminosilicate sample (Siral 60) in 1,2-dichloroethane at room temperature. It should be noted that the triphenylmethylium UV/vis absorption at  $\lambda = 412/435$  nm was clearly observed for each sample.

formation in the particle suspension. It should be also noted in the case of the silicas that a desorption of some surface-generated  $(\text{C}_6\text{H}_5)_3\text{C}^+$  takes place into the surrounding solvent phase of dichloromethane. This reaction is observable by the characteristic UV/vis absorption of  $(\text{C}_6\text{H}_5)_3\text{C}^+$  in the supernatant solvent phase. The desorption process is caused by HCl that is formed by reaction of the chloride ion with a very small fraction of rather acidic silanols. A consecutive reaction of HCl with an excess of  $(\text{C}_6\text{H}_5)_3\text{CCl}$  gives  $(\text{C}_6\text{H}_5)_3\text{C}^+ \text{HCl}_2^-$ . This reaction was only observed for the pure silicas and was also found to be dependent on the acidity of the silica (see also experimental part).<sup>47b</sup>

Despite the result that the UV/vis absorption maximum of the chemisorbed triphenylmethylium is unchanged by the nature of the solid acid catalyst, the corresponding fluorescence spectra show a dependence of the emission maximum on them (see Figure 2a).

Triphenylmethylium hexachloroantimonate  $[(\text{C}_6\text{H}_5)_3\text{C}^+ \text{SbCl}_6^-]$  is usually not fluorescent in 1,2-dichloroethane solution at room temperature. Since the rotational and vibrational motions of the  $(\text{C}_6\text{H}_5)_3\text{C}^+$  molecule are restricted, it becomes fluorescent when encapsulated in zeolite supercages<sup>44,46</sup> or, as shown in this paper, adsorbed on the external surface of a solid acid catalyst. The shift of the emission maximum in the UV/vis spectrum ranges from  $\lambda = 509$  nm (silica gel LC 1500) to  $\lambda = 555$  nm (alumina). In contrast to the significant influence of the nature of the solid acid on the position of the emission maximum of adsorbed  $(\text{C}_6\text{H}_5)_3\text{C}^+$ , an influence of the kind of the precursor,  $(\text{C}_6\text{H}_5)_3\text{COH}$ ,  $(\text{C}_6\text{H}_5)_3\text{CCl}$ ,  $(\text{C}_6\text{H}_5)_3\text{CNCS}$ , or  $(\text{C}_6\text{H}_5)_3\text{CBr}$ , is not observed (Figure 2b). This shows that the electronic structure and perhaps also the reactivity of the carbenium are mainly modified by the solid acid catalyst.<sup>52</sup>

A quantitative determination of the true concentration of the chemisorbed triphenylmethylium cations per square meter of

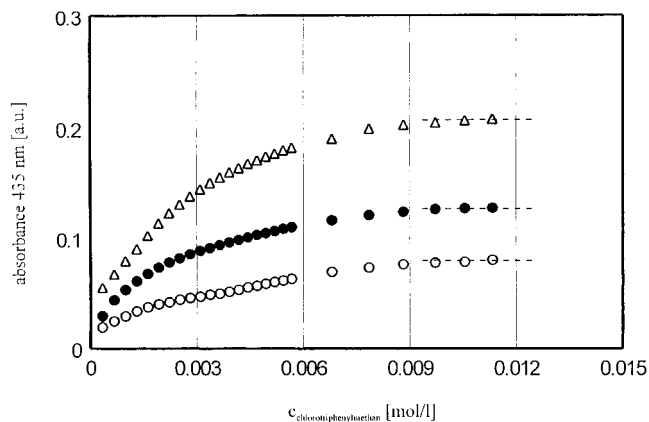


**Figure 3.** Relative intensity of the triphenylmethylium UV/vis absorption band at  $\lambda = 435$  nm, measured on Aerosil 300 in a continuously stirred slurry using dichloromethane as solvent by the transmission mode, as a function of the overall concentration of chlorotriphenylmethane for three different amounts of Aerosil 300 used: (○) 0.3208, (●) 0.475, and (△) 0.793 g.

the solid acid is difficult to achieve because the molar absorption coefficient of the  $(\text{C}_6\text{H}_5)_3\text{C}^+$  surface species is different from the value observed in regular solvents. The absorption coefficient of triphenylmethylium is about  $\epsilon = 38\,500\text{--}40\,000 \text{ L}\cdot\text{mol}^{-1}\cdot\text{cm}^{-1}$  at 412/435 nm in 1,2-dichloroethane or dichloromethane.<sup>53</sup> Because Aerosil 300/1,2-dichloroethane (DCE) as well as Aerosil 300/dichloromethane suspensions are absolutely transparent, the absorption intensity of chemisorbed triphenylmethylium was measured as a function of chlorotriphenylmethane concentration in a continuously stirred slurry under reproducible and inert conditions. For reproducible measurements, a rather high amount of Aerosil 300 particles is required in order to get a sufficient and constant concentration of the Aerosil 300 particles in the slurry.

Results of the quantitative triphenylmethylium measurements on three different amounts of Aerosil 300 particles are shown in Figure 3. The UV/vis spectrum of the slurry was recorded immediately after the stock solution of  $(\text{C}_6\text{H}_5)_3\text{CCl}$  was added to the Aerosil 300 suspension. The adsorption process occurs immediately as shown by the very rapid increase of the triphenylmethylium UV/vis absorption at  $\lambda_{\text{max}} = 435$  nm. The time required for mixing the components determines the rate of ionization. That is an indication that the rate of the adsorption–ionization process of  $(\text{C}_6\text{H}_5)_3\text{CCl}$  is controlled by the rate of its diffusion to the particle surface.

For each amount of the solid acid used, the triphenylmethylium concentration approaches a constant value that increases with the chlorotriphenylmethane concentration. This is consistent with both the existence of a real equilibrium between the amount of  $(\text{C}_6\text{H}_5)_3\text{CCl}$  in solution and on the surface and with the formation of a triphenylmethylium layer according to a Langmuir isotherm plot. It should be noted that this behavior is not generally observed for the adsorption of  $(\text{C}_6\text{H}_5)_3\text{CCl}$  on solid acids. For MCM-41 at higher  $(\text{C}_6\text{H}_5)_3\text{CCl}$  concentrations, multilayers are partly detectable.<sup>54</sup> However, the concentration of triphenylmethylium ions in the particle suspension depends linearly on the amount of the solid acid. That can be shown by the experimentally obtained dependence of the intensity of the triphenylmethylium absorption on the total surface area  $A$  expressed as  $\text{m}^2$ .  $A$  is the product of the amount of Aerosil 300 used and its specific BET surface area (Figure 4).

Since an excess of  $(\text{C}_6\text{H}_5)_3\text{CCl}$  is used for the model reaction, for each fixed amount of the solid acid catalyst a specific

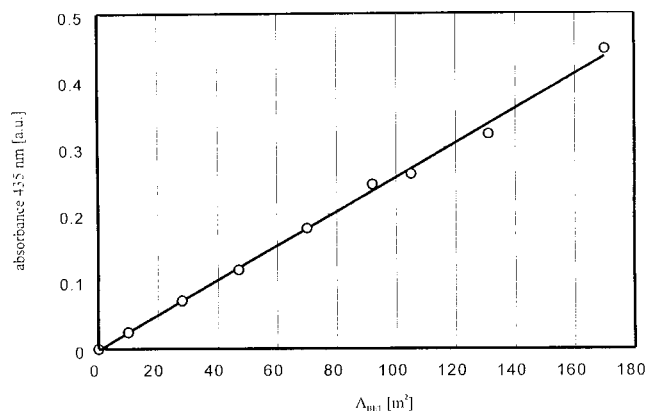


**Figure 4.** Relative intensity of the triphenylmethyl cation UV/vis absorption at  $\lambda = 435$  nm, measured on Aerosil 300 in a continuously stirred slurry of dichloromethane by the transmission technique at room temperature, as a function of the corresponding surface area per square meter of the amount of the solid acid used.  $[(C_6H_5)_3CCl] = 0.01189 \text{ mol} \cdot L^{-1}$  in dichloromethane.

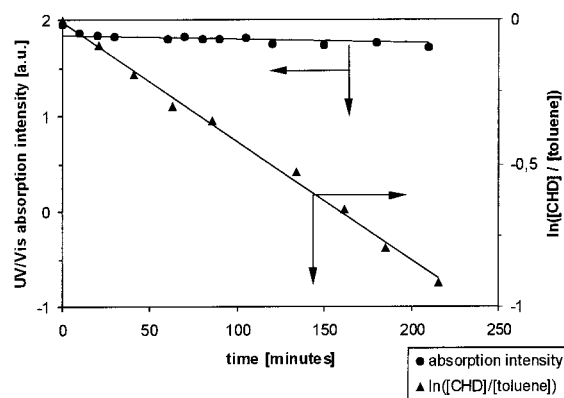


**Figure 5.** Intensity (●) of the triphenylmethyl cation UV/vis absorption at  $\lambda = 435$  nm, measured on a silica powder (KG 60 from Merck) in a continuously stirred slurry of dichloromethane by the transmission technique at room temperature, as function of the reaction time  $t$  (in min) during the model reaction. The other curve shows the corresponding kinetic plot  $\ln\{[CHD(t)]/[CHD(0)]\}$  (▲) of conversion of CHD to benzene during this reaction.

concentration of the reactive species, the triphenylmethyl cation, should be present.

**Kinetic Measurements.** Generally, for the polar reaction of a nucleophile with an electrophile, the following rate law is valid as shown for the reaction of CHD with  $(C_6H_5)_3C^+$  (eq 3).<sup>55</sup>



The quantitative UV/vis measurements showed that for each fixed amount of the solid acid, with an excess of the precursor  $(C_6H_5)_3CCl$ , a constant concentration of the relevant surface species should be present. The concentration of  $(C_6H_5)_3C^+$  is constant during the conversion of CHD when reacted  $(C_6H_5)_3C^+$  is immediately regenerated by rechemisorption of  $(C_6H_5)_3CCl$ . This is because the adsorption–ionization process of  $(C_6H_5)_3CCl$  to the solid acid is very rapid and, therefore, not the rate-determining step. This important assumption was supported by the measured intensity of triphenylmethyl cation on the surface of the solid acid catalyst during the hydride-transfer reaction. Figure 5 shows both the intensity of the triphenylmethyl cation UV/vis absorption at  $\lambda = 435$  nm and the kinetic plot for the conversion of CHD to benzene as a function of the reaction time.

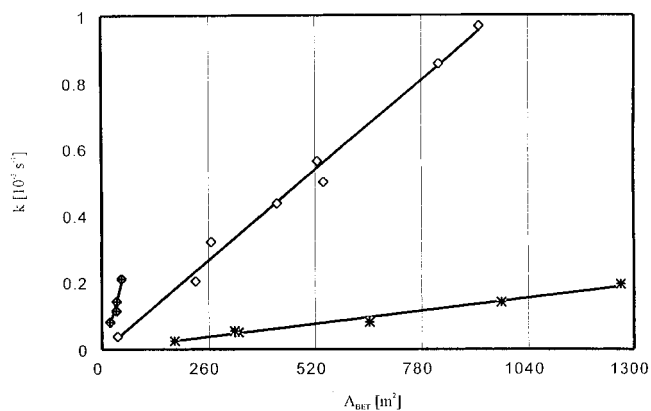


**Figure 6.** Correlation of the pseudo-first-order rate constant ( $k$  in  $s^{-1}$ ) of the hydride-transfer reaction of CHD with triphenylmethyl cation as function of the corresponding surface area ( $A$ ) per square meter of each solid acid catalyst used: (\*) silica gel KG 60, (◆) alumina, and (◇) aluminosilicate Siral 80.  $[(C_6H_5)_3CCl] = 0.5 \text{ g}$ ,  $[CH_2Cl_2] = 25 \text{ mL}$ ,  $T = 295 \text{ K}$ .

In the first stage of the reaction, between 5 and 50% conversion of CHD, the assumed condition is exactly met. In the second stage of the reaction, the deviation from the theoretical line is not important.

Thus, the product of  $k_2$  ( $L \cdot mol^{-1} \cdot s^{-1}$ ) and  $[(C_6H_5)_3C^+]$  ( $mol \cdot L^{-1}$ ) can be expressed as the pseudo-first-order-rate constant  $k$  ( $s^{-1}$ ) when an excess of the triphenylmethyl cation precursor is used. This reduces eq 3 to eq 4.

$$-d[CHD]/dt = k[CHD] \quad (4)$$

A pseudo-first-order kinetic model of the reaction with respect to the conversion of CHD or formation of benzene (B) was experimentally verified for each solid acid catalyst. Figure 5 is an example using silica. Both slopes  $-\ln[C_{CHD}(t)/C_{CHD}(0)]$  and  $\ln[C_B(t)/C_B(0)]$  as functions of time ( $t$ ) give first-order rate constants within the error of measurement. The kinetic plots are linear up to 70–90% conversion of CHD for each case.

The pseudo-first-order rate constant of this reaction—found by using constant concentrations of  $(C_6H_5)_3CCl$  and CHD—increases linearly with the amount ( $m$ ) of the solid acid catalyst used. Each amount ( $m$ ) corresponds to a specific area in square meters ( $A$ ) of the solid acid catalyst. This can also be expressed using the BET surface area by nitrogen adsorption as the reference system for the solid acid;  $m \text{ (g)} \times \text{BET (m}^2 \text{ g}^{-1}) = A \text{ (m}^2\text{)}$ . Measured  $k$  values as a function of the total surface area ( $A$ ) of the solid acid catalyst are shown in Figure 6 for three different solid acid catalysts.

As can be seen from Figure 6,  $k$  (eq 4), for the hydride-transfer reaction of CHD with chemisorbed  $(C_6H_5)_3C^+$ , strongly depends on the nature of the solid acid catalyst used. The linear plots obtained in Figure 6 support both the kinetic approach and the catalytic activity to be required from the solid acid for this reaction. Thus, for each plot and, therefore, for each solid acid catalyst, a specific rate constant  $k'$  ( $s^{-1} \text{ m}^{-2}$ ) can be calculated with respect to the surface area (eq 5).

$$dk/dA = k' \quad (5)$$

Consequently, the  $k'$  value is a complex quantity that involves the second-order rate constant ( $k_2$ ) of the elementary step and the concentration of  $(C_6H_5)_3C^+$  per square meter of the solid acid catalyst.

The measured  $k'$  values for the model reaction, the Kamlet–Tafts polarity parameters  $\alpha$ , and  $\pi^*$ , Gutmans acceptor number

**TABLE 2: Calculated  $\alpha$  and  $\pi^*$  Values, Measured  $E_T(30)$  Values, and Relative Rate Constants of the Model Reaction  $\log k'$  for the Solid Acid Catalysts**

sample no.	$\alpha_1$	$\alpha_2$	$\pi^*_{11}$	$\pi^*_{12}$	AN	$E_T(30)$ measured (kcal mol <sup>-1</sup> ) (eq 1a)	$\log k'$
1	1.13		1.08		49.4	58.1	-6.95
2	1.14		0.98		49.7	57.9	-6.48
3	1.25		1.00		53.2	58.5	-5.97
4	1.05				46.3	59.6	-7.20
5	1.14		1.00		49.7	58.1	-6.68
6	1.41	1.28	0.49	2.49	57.3	57.3	-5.57
7	1.57	1.16	0.31	1.72	60.3		-5.41
8	1.53	1.40	0.33	2.47			-5.79
9	1.12		0.56		48.2	55.8	-6.02
10	1.67		0.35		65.1	59.1	-5.33
11	1.36		0.45		55.6	62.6	-5.82
12	1.69		0.36		65.6	62.8	-5.71
13	1.77		0.38		68.4		-5.52
14	1.66	1.54	0.48	2.33	65.1	60.8	-5.72
15	1.80	1.67	0.45	2.47	59.5		-5.50
16	1.56	1.31	0.50	1.37	61.89		-5.83
17	1.50	1.24	0.54	1.44	60.3		-5.48
18	1.55	1.31	0.56	1.37	61.89		-5.52
19	1.50	1.15	0.40	1.61	58.74		-5.60
20	1.40	1.10	0.57	1.62	57.19		-5.56
21	1.40	1.30	1.07	1.40	61.89		-5.48
22	1.78	1.45	0.27	1.41	66.75		-5.36
23	1.38	1.47	0.61	2.41	62.88		-5.73
24	1.35	1.22	0.59	2.57	55.61	59.5	-5.90
25	1.35	1.23	0.68	2.53	55.61	54.2	-5.98
26	1.48	1.37	0.95	2.53	60.27	63.5	-5.41
27	1.60		0.71		63.40		-5.47
28	1.44		0.73		58.77	59.7	-5.61
29	1.73		0.49		67.26		-5.64
30	1.77				68.9		-5.82
31		0.90		2.84		45.9	-6.29
32	1.58		0.61		62.88	61.60	-5.78
33	1.61		0.68		63.97		-5.51
34	1.53		0.60		61.37	61.20	-5.67
35	1.38		0.66		56.40		-5.53
36	1.40	1.24	0.16	2.52	56.20	55.30	-5.68

AN, and Reichardt's  $E_T(30)$  values for the solid acids are compiled in Table 2.

As expected, significant differences in the catalytic activity are observed for the different silicas, aluminas, titanium dioxides, and aluminosilicates as well as for the alumina-functionalized silicas. The lowest reactivities are found for the silicas, the largest reactivities for the aluminas and titanium dioxides. Measurable differences of catalytic activity between the different silica samples are evident.

## Discussion

According to the theory of the solvatochromic measurements,<sup>20,21</sup> the differences of the UV/vis absorption energies of the solvatochromic dyes have been used as the quantity for determining the surface polarity parameters. For this reason the logarithm of the rate constants should be used for linear correlation analyses between the polarity parameters and the kinetic parameter  $k'$ .<sup>55,56</sup>

An important question remained from our previous paper. Is it justifiable to separate the part of the  $\pi^*$  term from the  $\nu_{\max}(2)$  value using simultaneously the measured  $\nu_{\max}(3)$  of adsorbed **3**.<sup>22c</sup> Because of the multiple adsorption mechanism of **3** toward surfaces of solid acids containing both Lewis and Brønsted acid sites, it is still not clear whether the two indicators adequately reflect the polarity values of a surface site.

As shown in the previous paper,<sup>22c</sup> the surface polarity indicator **2** cannot distinguish between Brønsted and Lewis acid

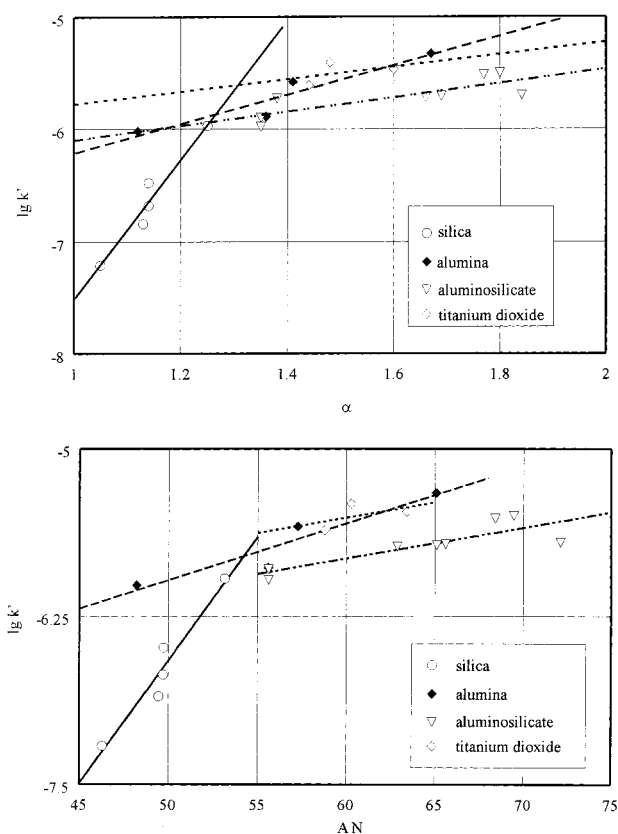


**Figure 7.** (a, top) Relationships between the relative rate constant of the model reaction ( $\log k'$ ) and the Kamlet–Taft  $\alpha$  value of solid acid catalysts: (○) silicas, (▽) aluminosilicates; (●) aluminas, and (◇) titanium dioxides. (b, bottom) Relationships between the relative rate constant of the model reaction ( $\log k'$ ) and Gutmann's acceptor number AN of solid acid catalysts: (○) silicas, (▽) aluminosilicates, (●) aluminas, and (◇) titanium dioxides.

sites. Using only its absorption maximum [ $\nu_{\max}(2)$ ] when **2** is adsorbed onto the solid acid, the acceptor number (AN) of Gutmann can be easily calculated by eq 6.<sup>57</sup> Equation 6 was derived from a data set of 27 various nonprotic and protic solvents.<sup>25a</sup>

$$\text{AN} = \{ \nu_{\max}(2) \times 10^{-3} [\text{cm}^{-1}] - 15.17 \} / 0.073 \quad (6)$$

$$n = 27, \quad r = 0.976, \quad \text{sd} = 1.12$$

AN values for solid acids can be easily calculated from the  $\nu_{\max}(2)$  values from ref 22c and by eq 6.<sup>25a</sup> As mentioned, the AN as well as the  $\nu_{\max}(2)$  is a complex quantity involving both the  $\alpha$  and  $\pi^*$  terms of an environment or a relevant surface site.<sup>25,28a</sup> This is shown in eq 7.<sup>25a</sup>

$$\nu_{\max}(2) = 14.94 + 2.24\alpha + 1.63\pi^* \quad (7)$$

$$n = 34, \quad r = 0.961, \quad \text{sd} = 0.316$$

The  $\alpha$  term contributes about 74% to the quantity  $\nu_{\max}(2)$  measured in a wide range of solvent polarities. The determination of the  $\alpha$  value by means of correlation analyses of the solvatochromism of the indicators **2** and **3** gives an equation where  $\nu_{\max}(2)$  determines the value of the  $\alpha$  term to about 95%.<sup>22c</sup> Therefore, it makes no significant difference as to which term, AN or  $\alpha$ , is used for the following discussion. Figure 7 shows the plots of the  $\log k'$  values as a function of the Kamlet–Taft  $\alpha$  value (Figure 7a) and AN values (Figure 7b) for the solid acid catalysts. As expected, Figure 7a appears almost identical to Figure 7b.

**TABLE 3: Calculated Equations for log  $k'$  versus the Polarity Parameters AN,  $\alpha$ ,  $\pi^*$ , and  $E_T(30)$  for the Solid Acid Catalysts Used in This Paper**

eq no.	calcn for	$\log k' = a\alpha + b\pi^* + cAN + dE_T(30) + e$					$n$	$r$	sd
		$a$	$b$	$c$	$d$	$e$			
8	all samples			0.0445		-8.494	20	0.740	
9	silicas			0.183		-15.73	5	0.968	
10	aluminosilicates			0.023		-7.198	8	0.850	
11	alumina			0.0424		-8.101	4	0.943	
12	silicas	6.26				-13.78	5	0.972	
12a	aluminosilicates	0.629				-6.73	8	0.807	
12b	alumina	1.298				-7.509	4	0.940	
13	all samples				0.0348	-8.022	18	0.270	0.507
14	all samples ( $\alpha_1, \pi^*_1$ )	1.229	-0.234			-7.403	32	0.746	0.250
15	all samples ( $\alpha_2, \pi^*_2$ )	0.614	-0.287			-5.848	17	0.791	0.153
16	all samples ( $\alpha_{1or2}, \pi^*_{1or2}$ )	0.967	0.112			-7.214	32	0.517	0.322

The results of the multiple least-squares analysis for log  $k'$  versus the polarity parameters are compiled in Table 3.

The correlation equation log  $k'$  as a function of AN for the titanium dioxides was not calculated because only three different samples were used. Alumina-functionalized silicas show a very poor correlation for log  $k' = f(AN)$  because their catalytic activity and polarity parameters do not vary significantly with surface composition.

The five different silica samples give an excellent correlation between their catalytic activity and the corresponding values of AN (eq 9) or  $\alpha$  (eq 12).

The aluminosilicates and several aluminas also show separate correlations of the log  $k'$  value with the  $\alpha$  value as similarly observed for the AN values.

It is evident that the different aluminas, titanium dioxides, and aluminosilicates are not as different in their catalytic activity as their  $\alpha$  values would predict. For the silicas, small variations in the value of the  $\alpha$  term are reflected strongly in their catalytic activity.

As mentioned, the  $k'$  value involves both the rate constant  $k_2$  of the elementary step and the concentration of immediately generated triphenylmethyl cation per square meter of solid acid catalyst. Therefore, both options, the variation of either the elementary step or the concentration of triphenylmethyl cation, depending on the nature of the solid acid catalyst, must be considered in interpretation of the results.

For the model reaction in dichloromethane, the rate constant ( $k_2$ ) of the elementary step of CHD to  $(C_6H_5)_3C^+$  was determined to be  $0.317 \pm 0.006 \text{ L mol}^{-1} \text{ s}^{-1}$  at 22 °C by Mayr and Lang.<sup>39</sup> Assuming this value is constant and independent of the solid acid catalyst, a surface concentration for  $(C_6H_5)_3C^+$  of  $c = 1.27 \times 10^{-4} \text{ mol} \cdot \text{L}^{-1}$  was estimated for  $m = 1 \text{ g}$  of Aerosil 300 in dichloromethane using  $[(C_6H_5)_3C^+] = (k' \cdot \text{BET} \cdot m) / k_2$ , with the measured BET surface for Aerosil 300 =  $240 \text{ m}^2 \text{ g}^{-1}$ . This model calculation is only justified for Aerosil 300 because the intensity of the UV/vis spectrum of chemisorbed  $(C_6H_5)_3C^+$  is reproducibly measurable in transmission mode for Aerosil 300 in dichloromethane.

A  $(C_6H_5)_3C^+$  concentration of  $1.2 \times 10^{-5} \text{ mol} \cdot \text{L}^{-1}$  per gram of Aerosil 300 can be independently calculated for the solid using the absorption intensity values.<sup>53</sup> That the kinetic approach gives a larger surface concentration of  $(C_6H_5)_3C^+$  than does the UV/vis technique is expected because the density of the Aerosil 300 particles in the dichloromethane slurry used for the UV/vis measurement is slightly lower than required to treat the slurry like a liquid. Despite the assumptions made for the estimation, the order of magnitude derived from the kinetic

experiment and UV/vis spectroscopy is satisfactory. The difference between the two methods can also be explained by the following arguments. The UV/vis absorption coefficients of  $(C_6H_5)_3C^+$  at  $\lambda = 435 \text{ nm}$  in solution and on the surface are probably not equivalent or the rate constant of the elementary step on the surface is about two to eight times larger than in the solvent dichloromethane. The rate constant of a polar reaction is only slightly dependent on the polarity of the environment; increasing the  $E_T(30)$  value of the solvent increases the second-order rate constant.<sup>55a</sup> The expected effect of the "solvent" polarity on  $k_2$  changing from dichloromethane [ $E_T(30) = 40.9$ ] to Aerosil 300/dichloromethane [ $E_T(30) = 58.5$ ] is five to eight times.<sup>55a</sup> That means the difference can also be explained in terms of the difference between the polarity parameters of pure dichloromethane and Aerosil 300 in dichloromethane. Of course, the influence of the catalyst environment on the benzenonium intermediate is ignored by this model calculation. Since the benzenonium intermediate is stabilized by the strong acid catalysts,  $Al_2O_3$  and aluminosilicates, the overall reaction rate should be reduced. Perhaps, the thermodynamic transition state of the CHD carbenium intermediate is responsible for the bend in the curve log  $k' = f(\alpha)$  (Figure 7a) because the dipolarity/polarizability term should more strongly affect the overall  $k$  value than does the acidity term  $\alpha$ .

Multiple correlation analyses of the log  $k'$  values with  $\alpha$  and  $\pi^*$  or with the directly measured  $E_T(30)$  values of the solid acids are also compiled in Table 3.

The correlation for the  $E_T(30)$  value is rather poor. For the multiple correlation using the  $\alpha_1$  and  $\pi^*_1$  values, an improved relation is obtained, compared to the single correlation log  $k' = f(\alpha)$  with  $r = 0.68$ . The improved correlation coefficient  $r$ , eq 14, shows that the  $\pi^*_1$  term has an influence on the overall rate of the reaction. The negative sign of the coefficient for the  $\pi^*$  suggests that a strong polarity retards the reaction rate, indicating a stabilization of the benzenonium intermediate.

In our previous paper we have also discussed that the indicator **3** (Michler's ketone) may be used to distinguish between Lewis and Brønsted acidic sites on the surface. Assumed  $\alpha$  and  $\pi^*$  values for the assigned Lewis sites, denoted as  $\alpha_2$  and  $\pi^*_2$ , were also reported in this paper.<sup>22c</sup>

Using these  $\alpha_2$  and  $\pi^*_2$  values of the aluminas, aluminosilicates, and titanium dioxides, which were calculated via the long UV/vis wavelength absorption of **3** at about  $\lambda = 500 \text{ nm}$ , an improved correlation (Table 3) for these solid acids (no.: 6–8, 14–26, 31, 36) is obtained. Equation 15 is satisfactory, and the coefficient for the  $\pi^*$  term also has a negative sign. By including all the solid acids when  $\alpha_2$  and  $\pi^*_2$  are used, rather



than  $\alpha_1$  and  $\pi^*$  for the samples (no.: 6–8, 14–26, 31, 36) as done by calculating eq 14, eq 16 is obtained. (Table 3) The fit of this multiple correlation eq 16 is rather poor.

We conclude that the  $\alpha$  term should be mainly responsible for the effective concentration of triphenylmethylum.

A significant influence of the pore diameter or the pore volume of the solid acid catalyst upon the rate constant is not detectable. Thus, transport processes should not be responsible for the effect observed.

In a following paper we will report on the influence of the counterion of the triphenylmethylum precursor counterion X [(C<sub>6</sub>H<sub>5</sub>)<sub>3</sub>C–X; X = Cl, OH, Br, NCS] and of substituents of the triphenylmethylum [(4–RC<sub>6</sub>H<sub>5</sub>)<sub>3</sub>C<sup>+</sup>, R = –OCH<sub>3</sub>, –Cl, –CH<sub>3</sub>] on the rate constant of the model reaction.<sup>58</sup>

## Conclusion

The results in this paper demonstrate that the Kamlet–Taft  $\alpha$  parameter or Gutman's AN is suitable to describe the catalytic activity of various moderately strong solid acid catalysts. They better describe surface reactivity for polar reactions as a surface polarity parameter than do single values of the  $E_T(30)$  or  $\pi^*$  parameter. In the range of  $\alpha = 1$  to  $\alpha = 1.9$  differentiating the surface acidity of moderately strong solid acids is better than using Hammett indicators. The method is especially useful for the characterization of different silica samples. We recommend especially the probe dye **2** as a surface polarity indicator to examine the Kamlet–Taft polarity parameter,  $\alpha$ , or Gutmann's AN of usual moderately strong solid acid catalysts.

These parameters can in turn be used to evaluate the catalytic activity of the catalysts. Despite the established correlation of the catalytic activity of solid acid catalysts with the value of the Kamlet–Taft  $\alpha$  parameter, further research is necessary for determining reliable values of the  $\pi^*$  parameter by independent model reactions that should not be significantly influenced by the surface acidity.

A fundamental question remains for the application of LSE approaches to study the surface polarity: are  $\pi^*$  and  $\alpha$  values to be mathematically orthogonal because rather complex properties of the surface influence the solvatochromic indicators that are adsorbed and then measured?

Despite these critical arguments, the method is very useful for rapidly characterizing the catalytic activity of weak and moderately strong solid acids.

**Acknowledgment.** Financial support in particular for this project by the Deutsche Forschungsgemeinschaft and the Fonds der Chemischen Industrie is gratefully acknowledged. We thank Condea GmbH, Merck AG Darmstadt, and Degussa for the samples of the solid acid catalysts. Mrs. Berger and Prof. D. Hoenicke, Department of Technical Chemistry, University of Technology, Chemnitz, performed the BET measurements.

## References and Notes

- (1) Corma, A. *Chem. Rev.* **1995**, 95, 559–614.
- (2) Olah, G. A. In *Acidity and Basicity of Solids, Theory, Assessment and Utility*; Fraissard, J., Petrakis, L., Eds.; NATO ASI Series 444; Kluwer Academic: Dordrecht, 1994; pp 305–334.
- (3) Corma, A. *Curr. Opin. Solid State Mater. Sci.* **1997**, 2, 63–75.
- (4) Bergna. In *The Colloid Chemistry of silica*; American Chemical Society: Washington, D.C., 1994; pp 1–47 and references therein.
- (5) Scott, R. P. W. *Silica Gel and Bonded Phases*; **1993**, John Wiley & Sons: New York, 1993.
- (6) Maciel, G. E.; Bronnimann, C. E.; Zeigler, R. S.; Sauer Chuang, J.; Kinney, D. R.; Keiter, E. A. In *The Colloid Chemistry of silica*; **1994**, American Chemical Society: Washington, D.C., 1994; pp 260–282.
- (7) Heeribout, L.; Semmer, V.; Batamack, P.; Dorémieux-Morin, C.; Vincent, R.; Fraissard, J. *Stud. Surf. Sci. Catal.* **1996**, 101, 831–840.
- (8) Chronister, C.; Drago, R. S. *J. Am. Chem. Soc.* **1993**, 115, 4793–4798.
- (9) Drago, R. S.; Dias, J. A.; Maier, T. O. *J. Am. Chem. Soc.* **1997**, 119, 7702–7710.
- (10) Drago, R. S.; Petrosius, S. C.; Chronister, C. W. *Inorg. Chem.* **1994**, 33, 367–372.
- (11) Xu, T.; Kob, N.; Drago, R. S.; Nicholas, J. B.; Haw, J. F. *J. Am. Chem. Soc.* **1997**, 119, 12231–12239.
- (12) Haw, J. B.; Nicholas, J. B.; Xu, T.; Beck, L. W.; Ferguson, D. B. *Acc. Chem. Res.* **1996**, 29, 259–267.
- (13) Drago, R. S.; Dias, S. C.; Torrealbe, M.; de Lima, I. *J. Am. Chem. Soc.* **1997**, 119, 4444–4452.
- (14) Umanski, P.; Engelhardt, J.; Hall, W. K. *J. Catal.* **1991**, 127, 128–140.
- (15) Fargasiu, D.; Ghenciu, A.; Li, J. Q. *J. Catal.* **1996**, 158, 116–127.
- (16) Dutta, P. K.; Turbeville, W. *J. Phys. Chem.* **1991**, 95, 4087–4092.
- (17) (a) Spange, S.; Reuter, A.; Schramm, A.; Reichardt, C. *Org. React. (Tartu)* **1995**. (b) Spange, S.; Reuter, A.; Vilsmeier, E. *Colloid Polym. Sci.* **1996**, 274, 59–69.
- (18) Taverner, S. J.; Clark, J. H.; Gray, G. W.; Heath, P. A.; Macquarrie, D. J. *J. Chem. Soc., Chem. Commun.* **1997**, 1147–1148.
- (19) Michels, J. J.; Dorsey, J. G. *Langmuir* **1990**, 6, 414.
- (20) Reichardt, C. *Solvents and Solvent effects in Organic Chemistry*; VCH: New York, 1988; p 21.
- (21) Reichardt, C. *Chem. Rev.* **1994**, 94, 2319.
- (22) (a) Spange, S.; Reuter, A. *Langmuir* **1999**, 15, 141–150. (b) Spange, S.; Reuter, A.; Lubda, D. *Langmuir* **1999**, 15, 2103–2111. (c) Spange, S.; Vilsmeier, E.; Zimmermann, Y. *J. Phys. Chem. B* **2000**, 104, 6417.
- (23) (a) Rutan, S. C.; Harris, J. M. *J. Chromatogr., A* **1993**, 656, 197–215. (b) Helburn, R. S.; Rutan, S. C.; Pompano, J.; Mitchern, D.; Patterson, W. T. *Anal. Chem.* **1994**, 66, 610.
- (24) (a) Reichardt, C.; Eschner, M. Unpublished results communicated to the editors. (b) Eschner, M. Ph.D. Thesis, Marburg, 1992.
- (25) (a) Spange, S.; Keutel, D. *Justus Liebigs Ann. Chem.* **1992**, 423. (b) Spange, S.; Keutel, D.; Simon, F. *J. Chim. Phys.* **1992**, 89, 1615.
- (26) Marcus, Y.; Migron, Y. *J. Phys. Org. Chem.* **1991**, 4, 310–315.
- (27) (a) Taft, R. W.; Kamlet, M. J. *J. Chem. Soc., Perkin Trans. 2*, **1979**, 1723. (b) Kamlet, M. J.; Abboud, J.-L. M.; Abraham, M. H.; Taft, R. W. *J. Org. Chem.* **1983**, 48, 2877.
- (28) Brune, B. J.; Payne, G. F.; Chaubal, M. V. *Langmuir* **1997**, 13, 5766.
- (29) Rutan, S. C.; Carr, P. W.; Taft, R. W. *J. Phys. Chem.* **1989**, 93, 4292–4297.
- (30) Park, J. H.; Carr, P. W. *J. Chromatogr.* **1989**, 465, 137–156.
- (31) Marcus, Y. *Chem. Soc. Rev.* **1993**, 409.
- (32) Novaki, L. P.; Soued, O. A. E. *Ber. Bunsen-Ges. Phys. Chem.* **1996**, 100, 8.
- (33) Spange, S.; Lauterbach, M.; Gyra, A. K.; Reichardt, C. *Justus Liebigs Ann. Chem.* **1991**, 323.
- (34) Lee, C.; Parrillo, D. J.; Gorte, R. J.; Farneth, W. E. *J. Am. Chem. Soc.* **1993**, 118, 3262–3268.
- (35) Barich, D. H.; Nicholas, J. B.; Xu, T.; Haw, J. F. *J. Am. Chem. Soc.* **1998**, 120, 12342–12350.
- (36) Leftin, H. P. *Carbonium Ions*; Olah, G. A., Schleyer, P. R., Eds.; John Wiley & Sons: New York, 1968; Vol. 1, p 363.
- (37) (a) Müller, P. *Helv. Chim. Acta* **1973**, 56, 1243. (b) Müller, P.; Joly, D. *Helv. Chim. Acta* **1983**, 66, 1110–1118.
- (38) (a) Spange, S.; Schmiede, B.; Walther, R. *GIT Fachz. Lab.* **1992**, 7, 736–737. (b) Spange, S.; Walther, R. *Org. React. (Tartu)* **1995**, 29, 45–48.
- (39) Mayr, H.; Lang, G. Unpublished results communicated to the editor. See also: Mayr, H.; Roth, M.; Lang, G. In *Cationic Polymerization, Fundamentals and Applications*; Faust, R., Sheffler, T. D., Eds.; ACS Symposium Series 665; American Chemical Society: Washington, D.C., 1977; pp 25–40.
- (40) (a) Weitz, E. *Chem. Ber.* **1939**, 72, 1740. (b) Weitz, E.; Schmidt, S. *Chem. Ber.* **1939**, 72, 2099.
- (41) Arai, H.; Saito, Y.; Yoneda, Y. *Bull. Chem. Soc. Jpn.* **1967**, 40, 312.
- (42) Karge, H. G. *Surf. Sci.* **1971**, 27, 419.
- (43) (a) Spange, S.; Fandrei, D.; Simon, F.; Jacobasch, H. *J. Colloid Polym. Sci.* **1994**, 272, 99–107. (b) Eismann, U.; Spange, S. *Macromolecules* **1997**, 30, 3439–3446. (c) Spange, S.; Eismann, U.; Höhne, S.; Langhammer, E. *Macromol. Symp.* **1997**, 126, 223–236.
- (44) Cano, M. L.; Corma, A.; Fornes, V.; Garcia, H.; Miranda, M. A.; Baerlocher, C.; Lengauer, C. *J. Am. Chem. Soc.* **1996**, 118, 11006–11013.
- (45) Cano, M. L.; Cozens, F. L.; Garcia, H.; Marti, V.; Scalano, J. C. *J. Phys. Chem.* **1996**, 100, 18152–18157.
- (46) Ramamurthy, V. *Surface Photochemistry* Anpo, M., Ed.; John Wiley & Sons Ltd.: New York, 1996; pp 65–115.
- (47) The degree of heterolytic dissociation of chlorotriphenylmethane on silica in a dichloromethane slurry is strongly temperature-dependent and reversible: with decreasing the temperature, the intensity of the visible

triphenylmethylium absorption increases three times from 20 to  $-75\text{ }^{\circ}\text{C}$ .<sup>49a,b</sup> Further information is available from the following e-mail address: stefan.spange@tu-chemnitz.de. (a) Eismann, U. Ph.D. Thesis, Chemnitz, 1996. (b) Zimmermann, Y.; Adolph, S.; Spange, S. Unpublished results.

(48) Baaz, M.; Gutmann, V.; Kunze, O. *Monatsh. Chem.* **1962**, 93, 1142–1161.

(49) Bentley, A.; Evans, A. G.; Halprem, J. *Trans. Faraday Soc.* **1951**, 47, 711–716.

(50) Schneider, S.; Mayr, H.; Plesch, P. H. *Ber. Bunsen-Ges. Phys. Chem.* **1987**, 91, 1369.

(51) Iliceto, A.; Fava, A.; Mazzuccato, V. *J. Org. Chem.* **1960**, 25, 1445.

(52) Xu, T.; Haw, F. *J. Am. Chem. Soc.* **1994**, 116, 10188–10195.

(53) Kalfoglou, N.; Sczwarc, M. *J. Chem. Phys.* **1968**, 72, 2233.

(54) Spange, S.; Graeser, A.; Rehak, P.; Jaeger, C.; Schultz, M. *Macromol. Chem. Rapid Commun.* **2000**, 21, 146–150.

(55) (a) Mayr, H. *Angew. Chem.* **1990**, 102, 1415–1428; *Angew. Chem., Int. Ed. Engl.* **1990**, 29, 1371–1384. (b) Mayr, H.; Patz, M. *Angew. Chem.* **1994**, 106, 990–1010; *Angew. Chem., Int. Ed. Engl.* **1994**, 33, 938–957. (c) Mayr, H.; Kuhn, O.; Gotta, M. F.; Patz, M. *J. Phys. Org. Chem.* **1998**, 11, 642–654.

(56) Funke, M.; Mayr, H. *Eur. J. Chem.* **1997**, 3, 1214–1222.

(57) Soukup, R. W.; Schmid, W. *J. Chem. Educ.* **1985**, 62, 459.

(58) Spange, S.; Adolph, S.; Walther, R. in preparation.